

Localized self-heating in large arrays of 1D nanostructures

Supplementary Information

O. Monereo,^a S. Illera,^a A. Varea,^a M. Schmidt,^b T. Sauerwald,^b A. Schütze,^b A. Cirera^a and J. D. Prades^a

^aMIND-IN2UB, Department of Electronics, University of Barcelona, 08028, Barcelona, Spain.

^bLab of Measurement Technology, Department of Mechatronics, Saarland University, 66123 Saarbrücken, Germany.

Sample Preparation

Sensor platforms formed by interdigitated Pt electrodes over a ceramic substrate fabricated by Francisco Albero S.A.¹ were used². The sensor platform included an embedded thermoresistance and a heater. Commercially available carbon nanofibers (CNFs), synthesized by means of CVD floating technique by Grupo Antolín S.A.³, were used. The fibers presented diameters ranging from 30 to 80 nm and lengths up to several μm . Additional details of this material can be found elsewhere⁴. CNFs were dispersed in 2-propanol at a concentration of 1 mg/ml. Then, the dispersion was drop-casted over the Pt electrodes. In Figure S.1 is shown an image of the film over the electrodes and a single CNF at different scales.

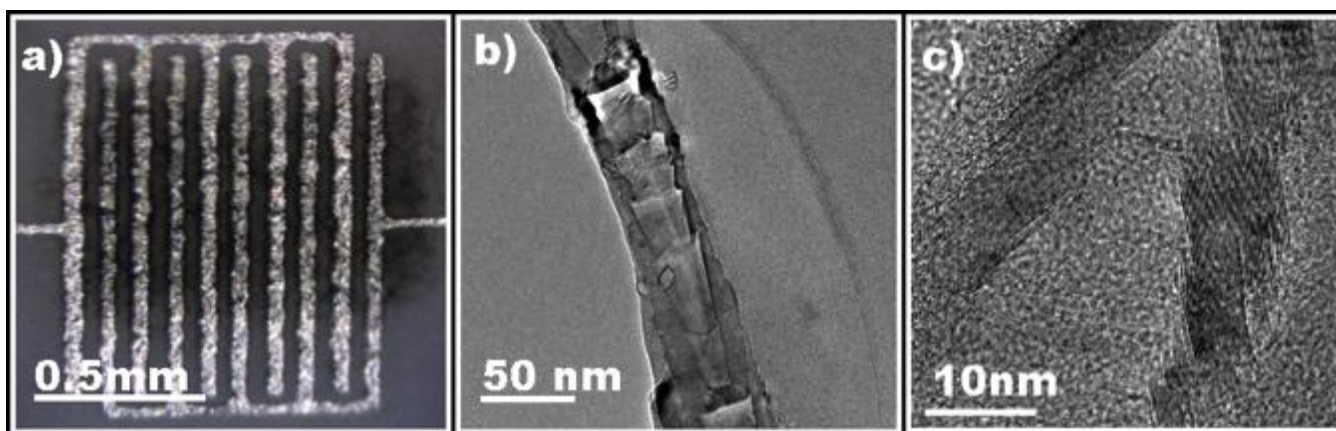


FIG. S.1 (a) Optical image of the carbon nanofibers (CNFs) film over the Pt electrodes. (b) Transmission electron microscope image of a single CNF and (c) transmission electron microscope image of a CNF at high resolution.

Electrical and thermographic measurements: experimental details

A two channel sourcemeter Keithley[®] Series 2602 SourceMeter was used for all electrical measurements, including heater powering and self-heating driving.

A thermographic camera ImageIR[®] 9300 was used for thermographic measurements.

Raman measurements: experimental details

For the Raman analyses, CNFs were deposited across the Pt electrodes forming one single conduction path, in order to guarantee that all the current flows through the observed region (Figure S.2).

Before the Raman measurements, the CNFs were annealed at 230 °C in nitrogen for 15 minutes using the heater embedded in the substrate and a gas tight chamber. The same chamber was equipped with an optical window. The nitrogen atmosphere was maintained with a flow rate of 200 ml/min during the Raman measurements to prevent any G band displacement due to gas molecules interaction (e.g. oxidizing species). After the first annealing process, the electrical film resistance decreased from (8.73 ± 0.01) k Ω to (8.12 ± 0.01) k Ω . Subsequent annealing processes in nitrogen lead to no significant change in the electrical resistance.

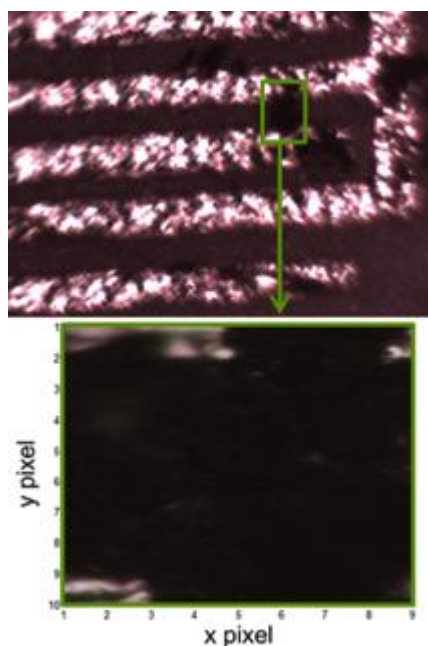


FIG. S.2 Optical image of the region analyzed by Raman spectroscopy. Pixel size are 5 and 3 μm for x and y spacing respectively.

Spatial Raman mappings were carried out using a Jovin Yvon HR800 LabRam. The laser excitation wavelength was set at 532 nm and a 50X long-working-distance objective was used. Laser power was set to 0.6 mW in all measurements in order to prevent laser-induced heating. The analyzed area was 30 x 50 μm^2 (see Figure S.2) and the corresponding pixel size was 3 μm by 5 μm in the x and y directions respectively. Each spectrum analyzed was the average of 5 different spectra acquired along 8 seconds. The baseline subtraction over the corresponding spectral range (1100 – 1800 cm^{-1}) and the G band position determination (1550 - 1600 cm^{-1}) for each pixel was extracted by MatLab[®] software following the procedure described elsewhere⁵.

The G band displacement due to temperature variations was calibrated for each analyzed pixel. For this, a first series of Raman mappings were acquired at room temperature and by applying different potentials (from 0.3 to 1.2 V with a potential step of 0.3 V) in heater operation mode. The heater operation assures a constant temperature for the entire sample, and a linear dependence between $\Delta\omega$ and T can be obtained for each pixel. To draw the temperature mappings distribution for self-heating process, a second series of Raman mappings were acquired. Different applied potentials (0, 3.2, 5.2, 6.2 and 8.2 V) were applied in self-heating operation. Then, the G band position displacement can be related with the local temperature value of each pixel by using the previously obtained calibration.

Electrical simulations

The electrical model is grounded on decomposing the wires in two different kinds of resistance contributions: contact and wire. Thus, the total resistance of the wire network includes contributions from the wire segments (R_w^i) and from the wire-to-wire contacts (R_c^j) in random combinations of series and parallel arrangements. Figure S.3(a) shows the electrical scheme of two example situations: one single wire connecting the two electrodes and two wires creating a contact node. The decomposition of the system in the different resistance elements is also shown. In real simulations, larger wire networks (more than 100 wires), such as the one shown in Fig. S.3(b) were used.

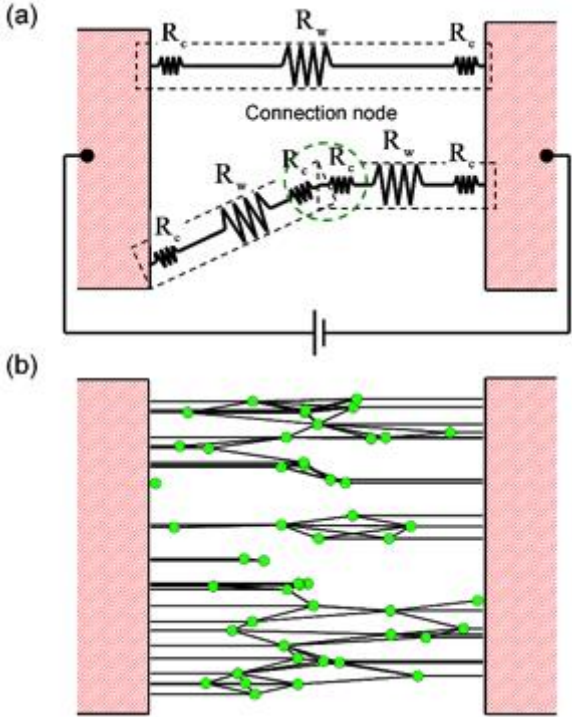


FIGURE S.3 (a) Basic electrical scheme of the system under consideration. The two electrodes (red squares) are bridged by three wires (dashed black boxes) randomly distributed. The wires are decomposed in three parts: two point contact resistances R_c at the ends, and a wire segment resistance R_w . In this example, there are two wires connected between them creating a point contact node (dashed green

circle). (b) Scheme of the simulated resistance network: the wires (black lines) are connected between them forming contact nodes (green circles) and to both electrodes (red blocks).

The simulations were performed under an external bias voltage $V = 2$ V. The distance between both electrodes was $40 \mu\text{m}$ and a uniform wire length of $20 \mu\text{m}$ was considered. The total equivalent circuit resistance and the total dissipated power are shown in Fig. S.4 for different α_R values. When α_R increases, the equivalent resistance also increases and the dissipated power decreases.

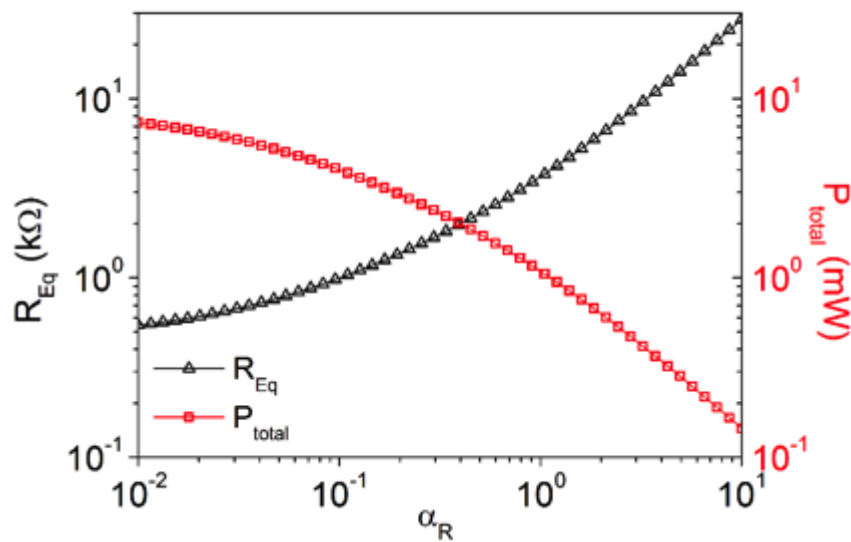


FIGURE S.4 Total equivalent resistance R_{Eq} and the total power P_{total} for different scale parameters.

References

- 1 FRANCISCO ALBERO S.A.U., Rafael Barradas, 19. Districte Econòmic Granvia L'H., 08908, Hospitalet de Llobregat, Spain.
- 2 F. M. Ramos, C. López-Gándara, A. Cirera and J. R. Morante, in *Proceedings of the 2009 Spanish Conference on Electron Devices*, 2009, pp. 293–296.
- 3 Grupo Antolín S.A., Ctra. Madrid-Irún, Km. 244,8 Apdo. 2069 B, 09007, Burgos.
- 4 J. Vera-Agullo, H. Varela-Rizo, J. A. Conesa, C. Almansa, C. Merino and I. Martin-Gullon, *Carbon N. Y.*, 2007, **45**, 2751–2758.
- 5 Z.-M. Zhang, S. Chen and Y.-Z. Liang, *Analyst*, 2010, **135**, 1138–46.